LA-UR- 10-03230

Approved for public release; distribution is unlimited.

Title: Diagnosing ICF Gamma-Ray Physics

Author(s): H.W. Herrmann, C.S. Young, J.M. Mack, Y.H. Kim, A. McEvoy, S. Evans, T. Sedillo, S. Batha, N. Hoffman, D.C. Wilson, J.R. Langenbrunner, W. Stoeffl, R. Malone, M.I. Kaufman, B.C. Cox, T.W. Tunnell, E.K. Miller, Z.A. Ali, C.J. Horsfield and M. Rubery

Intended for: 18th Topical Conference on High Temperature Plasma Diagnostics, Wildwood, NJ, May 16-20, 2010

Los Alamos
NATIONAL LABORATORY
EST. 1943

Diagnosing ICF Gamma Ray Physics

Author List

H.W. Herrmann, Y.H. Kim, A. McEvoy, C.S. Young, J.M. Mack, N. Hoffman, D.C. Wilson, J.R. Langenbrunner, S. Evans, T. Sedillo, S.H. Batha, L. Dauffy[a], W. Stoeffl[a], R. Malone[b], M.I. Kaufman[b], B.C. Cox[b], T.W. Tunnell[b], E.K. Miller[c], Z.A. Ali[d], C.J. Horsfield[e] and M. Rubery[e]

Los Alamos National Laboratory, P.O Box 1663, M/S E526, Los Alamos, NM 87545, USA
[a] *Lawrence Livermore National Laboratory, Livermore, CA 94550, USA*
[b] *National Security Technologies (NSTec), Los Alamos, NM 87544, USA*
[c] *NSTec, Special Technologies Laboratory, Santa Barbara, California, 93111 USA*
[d] *NSTec, Livermore, CA, 94550, USA*
[e] *Atomic Weapons Establishment, Aldermaston, Reading, RG7 4PR, UK*

Diagnosing ICF Gamma Ray Physics

H.W. Herrmann, Y.H. Kim, A. McEvoy, C.S. Young, J.M. Mack, N. Hoffman, D.C. Wilson, J.R. Langenbrunner, S. Evans, T. Sedillo, S.H. Batha, L. Dauffy[a], W. Stoeffl[a], R. Malone[b], M.I. Kaufman[b], B.C. Cox[b], T.W. Tunnell[b], E.K. Miller[c], Z.A. Ali[d], C.J. Horsfield[e] and M. Rubery[e]

Los Alamos National Laboratory, P.O Box 1663, M/S E526, Los Alamos, NM 87545, USA
[a] Lawrence Livermore National Laboratory, Livermore, CA 94550, USA
[b] National Security Technologies (NSTec), Los Alamos, NM 87544, USA
[c] NSTec, Special Technologies Laboratory, Santa Barbara, California, 93111 USA
[d] NSTec, Livermore, CA, 94550, USA
[e] Atomic Weapons Establishment, Aldermaston, Reading, RG7 4PR, UK

herrmann@lanl.gov

Gamma rays produced in an ICF environment open up a host of physics opportunities we are just beginning to explore. A branch of the DT fusion reaction, with a branching ratio on the order of 2e-5 γ/n, produces 16.7 MeV γ-rays. These γ-rays provide a direct measure of fusion reaction rate (unlike x-rays) without being compromised by Doppler spreading (unlike neutrons). Reaction-rate history measurements, such as nuclear bang time and burn width, are fundamental quantities that will be used to optimize ignition on the National Ignition Facility (NIF). Gas Cherenkov Detectors (GCD) that convert fusion γ-rays to UV/visible Cherenkov photons for collection by fast optical recording systems established their usefulness in illuminating ICF physics in several experimental campaigns at OMEGA. Demonstrated absolute timing calibrations allow bang time measurements with accuracy better than 30 ps. System impulse response better than 95 ps fwhm have been made possible by the combination of low temporal dispersion GCDs, ultra-fast microchannel-plate photomultiplier tubes (PMT), and high-bandwidth Mach Zehnder fiber optic data links and digitizers, resulting in burn width measurement accuracy better than 10 ps. Inherent variable energy-thresholding capability allows use of GCDs as γ-ray spectrometers to explore other interesting nuclear processes. Recent measurements of the 4.44 MeV $^{12}C(n,n')$ γ-rays produced as 14.1 MeV DT fusion neutrons pass through plastic capsules is paving the way for a new CH ablator areal density measurement. Insertion of various neutron target materials near target chamber center (TCC) producing secondary, neutron-induced γ-rays are being used to study other nuclear interactions and as in-situ sources to calibrate detector response and DT branching ratio. NIF Gamma Reaction History (GRH) diagnostics, based on the GCD concept, are now being developed based on optimization of sensitivity, bandwidth, dynamic range, cost, and NIF-specific logistics, requirements and extreme radiation environment. Implementation will occur in two phases: 1) four PMT-based channels mounted to the outside of the target chamber at ~6m from TCC (GRH-6m) for the 3e13-3e16 DT neutron yield range expected during the early ignition-tuning campaigns; and 2) several channels located just inside the target bay shield wall at 15 m from TCC (GRH-15m) with optical paths leading through the cement shield wall to well-shielded streak cameras and PMTs for the 1e16-1e20 yield range expected during the DT ignition campaign. Multiple channels at each phase will allow for increased redundancy, reliability, accuracy and flexibility. This suite of diagnostics will make possible exploration of interesting γ-ray physics well beyond the ignition campaign.

Introduction

Gamma-rays will be used to measure fusion reaction history on the National Ignition Facility (NIF) using gas Cherenkov detectors as part of the Gamma Reaction History (GRH) Diagnostics. This measurement is based on the 16.75 MeV gamma-ray resulting from a weak branch of the DT fusion reaction, having a branching ratio on the order of 2.5×10^{-5} gammas per DT neutron.

At ignition, DT neutron yields are expected to be on the order of 10^{19}. In order to tune the implosions toward ignition, NIF will be using THD (with a nominal ratio of 74/24/2) as a surrogate for 50/50 DT. This THD mixture maintains an implosion which is hydrodynamically equivalent to DT, while reducing neutron yields to the point where most diagnostics are still useful (e.g., $Y_{DTn} \sim 10^{14}$).

The GRH-6m will be located just outside the target chamber wall at approximately 6 m from target chamber center (TCC). It will be operable in the 10^{13}-10^{16} yield range. It consists of 4 gas cells which can be set to different gas pressures to achieve different Cherenkov energy thresholds. In this sense, it will be useful as a 4-channel, time-resolved, energy-thresholded, gamma-ray spectrometer.

The previous generation of gas Cherenkov detector (GCD) used to measure implosions on OMEGA could only obtain energy thresholds as low as ~6 MeV due to pressure and gas limitations. The new GRH diagnostics are designed to withstand higher pressure (up to 200 psia) and can be operated with SF6 in place of CO2. SF6, having a higher index of refraction than CO2, results in a lower energy threshold for a given pressure. At 200 psia of SF6, the lower limit in energy threshold is now approximately 3 MeV.

For direct-drive, DT implosions on OMEGA, the DT fusion gammas were essentially the only gamma-rays GCD was capable of measuring. Indirect-drive, THD implosions on NIF combined with the lower threshold capability of GRH opens up the possibility of detecting additional gamma-rays from which new information pertaining to the implosion effectiveness can be gleaned.

Expected NIF Gamma-Ray Spectra

Figure 1 depicts a calculated gamma-ray time history for neutron-induced secondary gammas from reactions of an instantaneous source of 14.1 MeV neutrons on the hohlraum of a NIF experiment. It assumes 0.9 scale flanged hohlraum with thermomechanical package (TMP) including silicon rings and arms. These secondary gammas peak about 60 ps after the DT gammas owing to the difference in time between fusion gammas and 14.1 MeV neutrons traveling the ~3 mm from tcc to the hohlraum walls. A second peak occurring about 0.25 ns after bang time, corresponds to the delay time to the hohlraum end caps located at ~1 cm. DT fusion gammas are depicted at t=0 at a level corresponding to the expected branching ratio of 2.5e-5 gammas/neutron. There are approximately 30 times more low-energy secondary gammas than there are DT fusion neutrons in this ½ ns window. The GRH has sufficient time response, and the expected reaction histories are short enough to be able to resolve any source of gammas beyond this time.

Figure 2 depicts the "prompt" gammas consisting of those generated from an instantaneous fusion reaction producing DT fusion gamma-rays at 16.75 MeV, HT fusion gamma-rays at 19.8

MeV, $^{12}C(n,n')$ gamma-rays at 4.43 MeV, and a continuum background of neutron-induced secondary gammas from reactions on the hohlraum within 0.5 ns after bang time (i.e., the integral of Figure 1). The spectrum is dominated by the $^{12}C(n,n')$ gammas created when 14.1 MeV neutrons inelastically scatter on their way through the plastic capsule ablator, and thus are directly related to the areal density of the capsule. This spectrum assumes an areal density of 500 mg/cm^2. The HT fusion reaction has a branching ratio of unity, forming a gamma-ray and a ^{4}He nucleus for every reaction. The expected HT gamma-ray yield is related to the DT gamma-ray yield by the ratio of their fusion cross sections at ~3 keV, their respective reactant concentrations, and their branching ratios.

$HTg/DTg = \langle\sigma v\rangle_{HT}[H][T]BR_{HT}/\langle\sigma v\rangle_{DT}[D][T]BR_{DT} \approx (4e\text{-}6*24)/(2*2.5e\text{-}5) \approx 2$

These fusion gamma-rays will be essentially time synchronous with the DT fusion gamma-rays, and thus can be used to boost the statistics of the bang time and burn width measurements.

The vertical axis on the right of the plot in Figure 2 shows the calculated response of the GRH in Cherenkov photons striking the photochatode of the PMT per gamma-ray incident on the 5" diameter convertor as a function of gamma-ray energy and threshold energy. The spectrum is binned in 100 keV bins, so the line widths are meaningless (the lines are drawn only to guide the eye). For example, at a gamma-ray energy of 20 MeV and a 3 MeV threshold energy, the GRH detects nearly as many Cherenkov photons as there are gamma-rays incident on the convertor. However, on average approximately 20 photons correspond to each detected gamma-ray, lowering the shot statistics.

The four GRH response curves correspond to the threshold energies we have chosen to best unfold the spectrum. Figure 3 shows the relative response at each of these thresholds where now the solid angle fraction of 2.71e-5 for a 5" diameter convertor placed 6.1 m from tcc is included to give the detector response in Cherenkov photons at the photocathode per source neutron for each 100 keV bin.

In Figure 4, the spectral responses as a function of threshold energy shown in Figure 3are integrated over the complete spectrum to give the expected GRH signal in Cherenkov photons striking the photocathode per source neutron. The signal drops by more than 2 orders of magnitude in going from the 3 MeV to the 14 MeV threshold energy. To have a statistically relevant signal, we typically desire at least 10^3 photons (correlating to approximately 50 detected gammas). Thus, at the highest threshold we intend to run, 14 MeV, a DT neutron yield of ~$3x10^{14}$ is desired.

Figure 5 shows the results of Figure 4 normalized by the total signal to show the contribution of each spectral component as a function of threshold energy. Without thresholding, only about 1% of gamma-rays are from fusion, and about 85% are from ^{12}C. At a threshold of 8 MeV, about 99% of the signal is from fusion (DT + HT). In order to be able to unfold the spectrum, thresholds are chosen at 3 and 5 MeV, which is just below and above the ^{12}C gamma-ray energy at 4.43 MeV. If one assumes the shape of the calculated hohlraum background continuum is roughly correct, then the 5 MeV measurement allows one to subtract the hohlraum contribution, along with the fusion contributions, from the 3 MeV signal, giving the $^{12}C\gamma$ signal. Another threshold is chosen at 14 MeV so as to separate the DT and HT components without suffering too much degradation in signal.

Given the measured signals at the four threshold energies and the relatively well known detector responses it is straight forward to solve for the four unknown yield contributions. This does require an assumed shape for the hohlraum spectrum, but the expected contribution is small enough that small errors in the shape aren't too significant in the analysis. It also requires well known detector responses which so far have been based on Monte Carlo simulations using the ITS-ACCEPT and GEANT4 codes. An extensive calibration run was conducted at the Duke University High Intensity Gamma-Ray Source (HIγS) in April, 2010, from which these calculations are being validated. HIgS provided a well characterized, 1 cm diameter pencil beam of gamma rays at flux levels of several 10^7 gammas/sec and three different beam energies (4.4, 10.0, & 16.8 MeV). Scans were performed in beam position and Cherenkov threshold energy (i.e., gas pressure) for the two different gases (CO2 & SF6) and various shielding configurations. These calibrations will significantly reduce the uncertainty in the responses, and hence in the yield contributions of the four spectral components.

Ablator Areal Density

Once the yield components are known, it is possible to infer several things about the implosions. First is the areal density, or $\rho_C R$, of the plastic ablator. Assuming a mono-energetic, instantaneous, point source (MIPS) model, the $\rho_C R$ can be expressed as:

$$< \rho_C R > \cong \frac{m_C}{\sigma_{nC}} \frac{Y_{\gamma C}}{Y_{nDT}}$$

where m_C is the mass of a carbon atom (12 amu), σ_{nC} is the cross section for inelastic scattering into the 4.44 MeV gamma, $Y_{\gamma C}$ is the yield of the 4.44 MeV gammas, and Y_{nDT} is the yield of the 14.1 MeV neutrons. The total neutron yield can be obtained from a neutron yield measurement, taking into account reduced flux at the detector due to downscattering, or from:

$$Y_{nDT} = Y_{\gamma DT} / B$$

where B is the DT branching ratio.

With direct-drive at OMEGA without any hohlraum contribution and without significant contribution from HT fusion in a DT capsule, the four signal equations reduce to just 2, and the expression for $\rho_C R$ becomes:

$$\left. \begin{array}{l} S_3 = R_{C,3} Y_{\gamma C} + R_{DT,3} Y_{\gamma DT} \\ S_5 = R_{C,5} Y_{\gamma C} + R_{DT,5} Y_{\gamma DT} \end{array} \right\} \Rightarrow \rho_C R = \frac{m}{\sigma} B \frac{R_{DT,3}}{R_{C,3}} \left[\frac{S_3}{S_5} \frac{R_{DT,5}}{R_{DT,3}} - 1 \right]$$

where S_{thr} is the measured signal for the specified threshold value, thr, and $R_{\gamma,thr}$ is the GRH response to the specified spectral component, γ, at the specified threshold, thr. The fact that $\rho_C R$ can be expressed as a product of ratios of signals and GRH responses means that the relative numbers factor into the uncertainty more than the absolute numbers. These ratios are better known than the absolutes. The biggest uncertainty comes from the Branching Ratio, which is currently uncertain to ~50%, but we have a campaign underway with a goal of lowering this uncertainty to <10%.

A simplified measurement of $\rho_C R$ took place using the GRH on OMEGA in October, 2009. This was the first time we had the capability to lower the threshold below the 4.44 MeV energy of the ^{12}C-γ. Since there is only one GRH channel on OMEGA, data were taken from successive shots with thresholds set above and below the 4.44 MeV ^{12}C-γ energy (3 and 4.6

MeV). The resulting $\rho_C R$ was ~30 mg/cm^2, consistent with expectations for these particular implosions. In May, 2010, similar more extensive measurements will be made including glass capsules as $\rho_C R$=0 controls, and with independent ρR measurements inferred from charged particle slowing down determined using wedge range filters and charged particle spectrometers.

Cold/Hot Fuel Mix

Another useful piece of information will be the HT to DT yield ratio. Although the implosions are intended to be nominally 74/24/2 in T/H/D ratio, the cryogenic layering process results in the heavier species, e.g., tritium, preferentially condensing out into the ice layer, leaving a tritium-poor/hydrogen-rich central gas region. The resulting gas composition ratio is expected to be closer to 18/81/1. As a result, the DT reactivity of the gas is reduced by a factor of ~8. However, a significant portion of the yield is expected to come from the inner surface of the ice layer, which maintains a composition closer to the intended 74/24/2. The more this cold inner layer mixes into the hot spot the more significant its contribution to the yield becomes, boosting the overall DT reactivity back up. Figure 6 shows the concentration products of D*T and H*T with normalization to one occurring at the initial 18% tritium in the hot spot. As the reacting concentration varies between that of the gas (18/81/2) and that of the bulk ice (74/24/2), the DT product increased by a factor of 8, while the HT product increases is much less affected. As a result, the yield ratio of the DT-γ to the HT-γ is a sensitive measure of the amount of mix occurring between the cold and hot fuel compositions.

Conclusion

The Gamma Reaction History diagnostics intended to be operated on the NIF will be capable of providing more than Reaction History components such as bang time and burn width. The use of multiple gas cells operating at independent threshold energies allows one to unfold the gamma-ray spectrum to obtain the yields of the individual components; specifically $Y_{\gamma DT}$, $Y_{\gamma HT}$, $Y_{\gamma C}$, and $Y_{\gamma Hohl}$ where a spectral shape is assumed for the hohlraum gamma-ray contribution. In addition to being useful quantities in themselves, these yields lead to inferences of ablator areal density and cold/hot fuel mix.

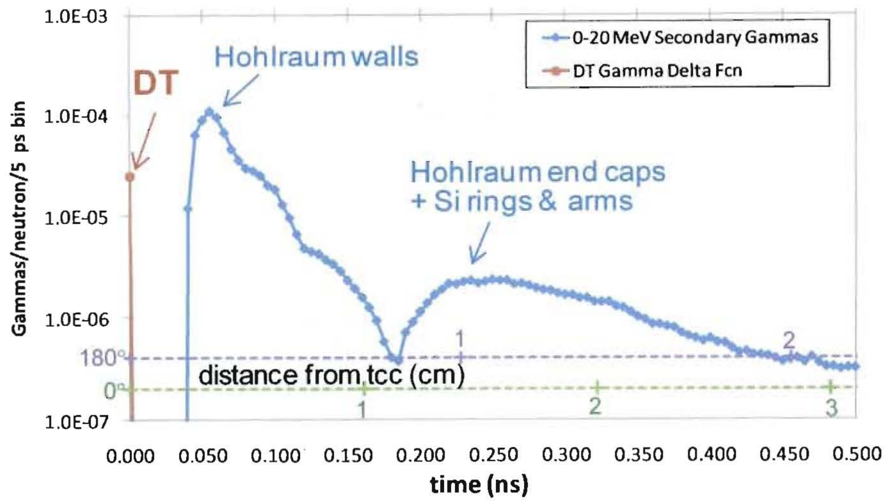

Figure 1

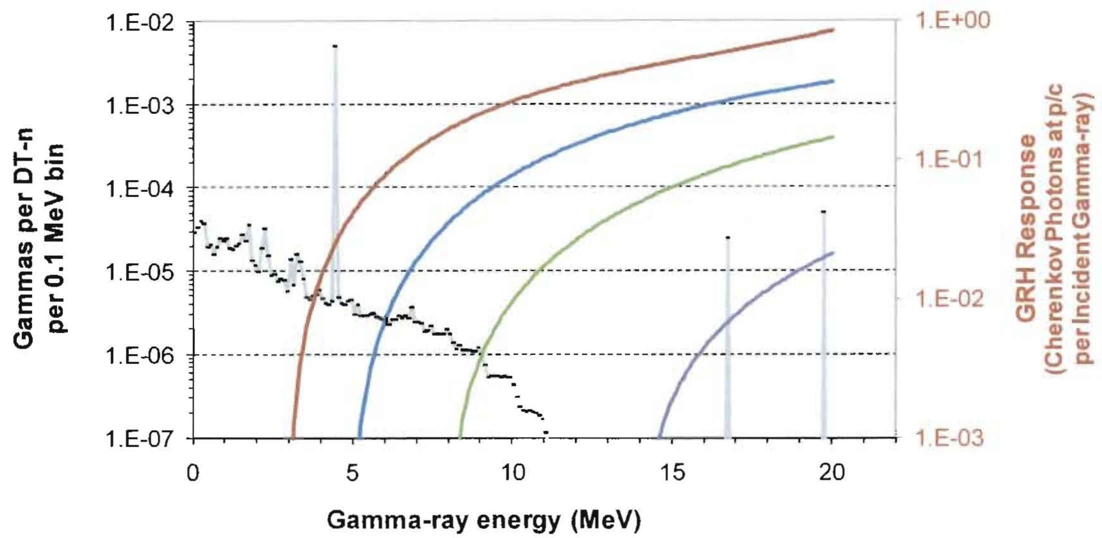

Figure 2

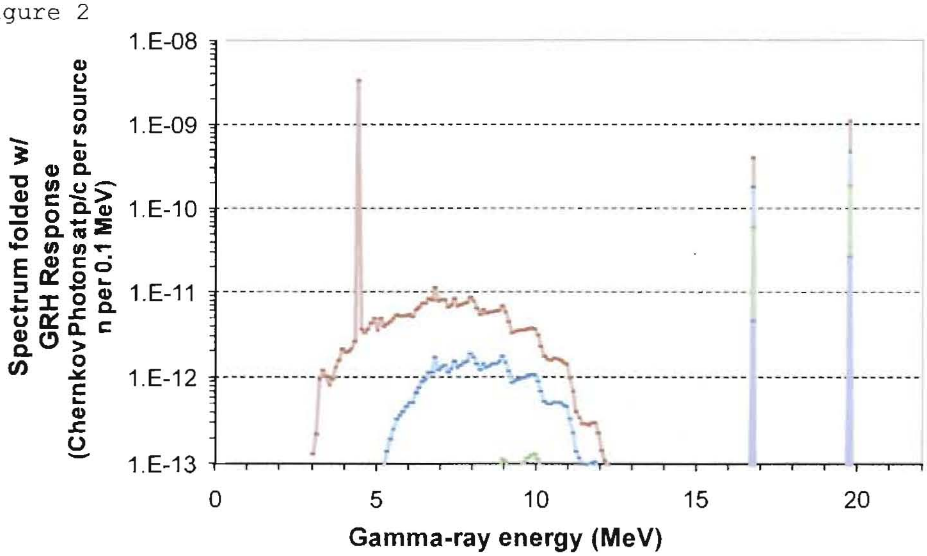

Figure 3

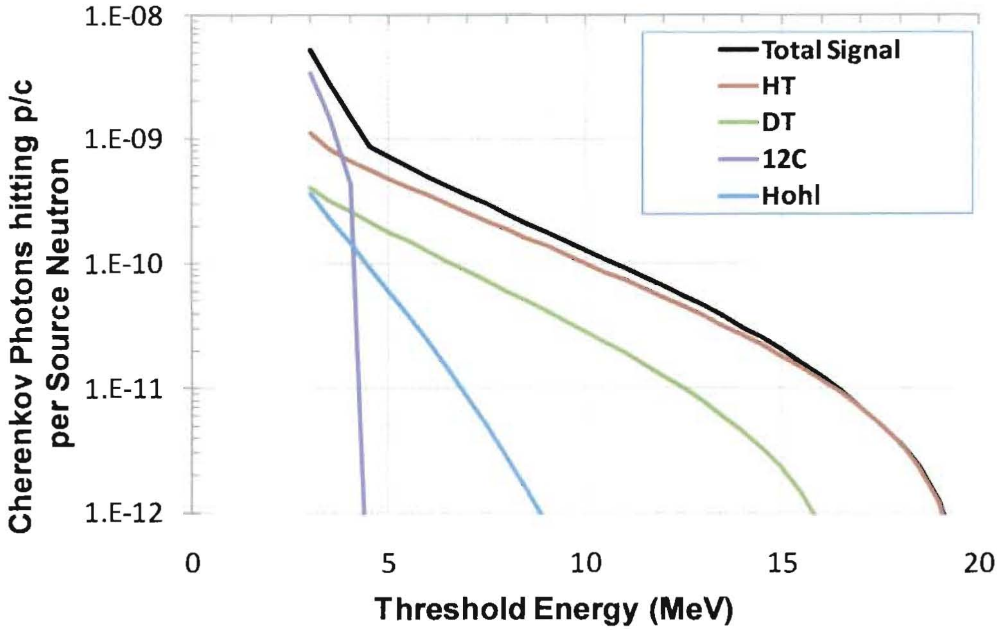

Figure 4

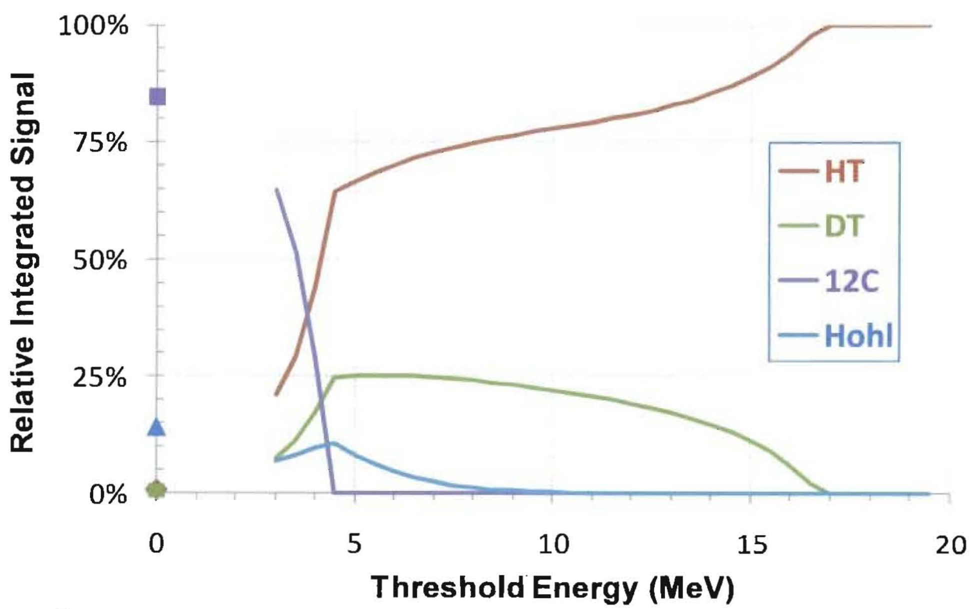

Figure 5

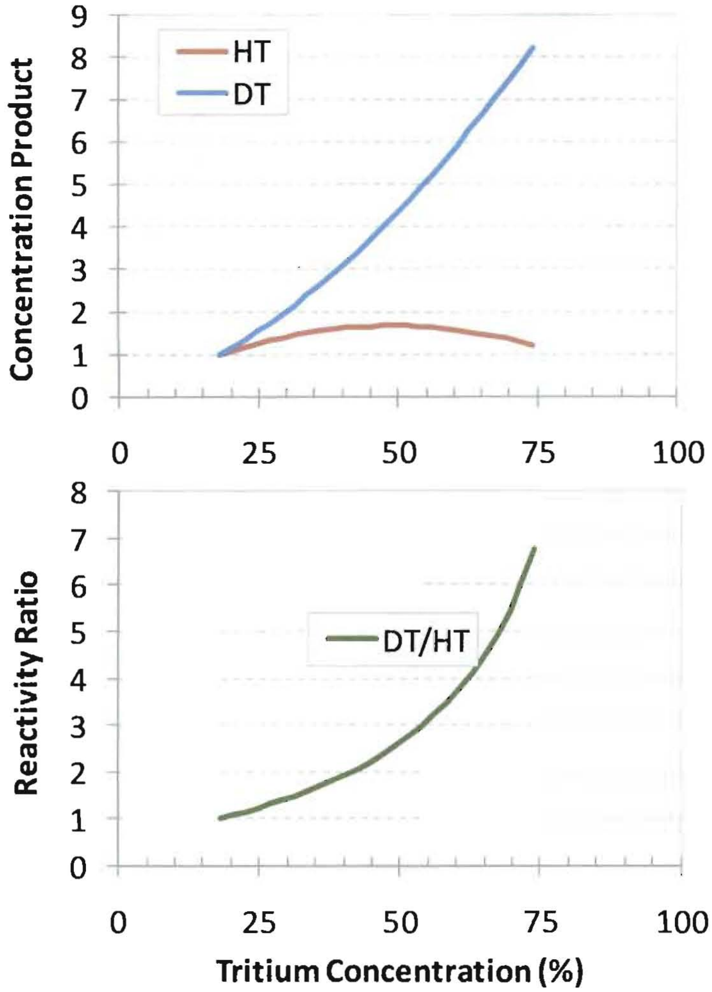

HT
DT
Concentration Product
DT/HT
Reactivity Ratio
Tritium Concentration (%)

Figure 6